https://doi.org/10.5194/egusphere-2023-2940
Preprint. Discussion started: 11 December 2023

The correlation between Arctic sea ice, cloud phase and radiation using A-train satellites

Grégory V. Cesana[1,2], Olivia Pierpaoli[3,2], Matteo Ottaviani[4,2], Linh Vu[3,2], and Zhonghai Jin[2]

[1]Center for Climate Systems Research, Columbia University, New York, NY
[2]NASA Goddard Institute for Space Studies, New York, NY
[3]Department of Atmospheric Sciences, University of Washington, Seattle, WA
[4]Terra Research Inc, Hoboken, NJ 07030

Correspondence: Grégory V. Cesana (gregory.cesana@columbia.edu)

Abstract. Climate warming has a stronger impact on Arctic climate and sea ice cover (SIC) decline than previously thought. Better understanding and characterizing the relationship between sea ice, clouds and the implications for surface radiation is key to improving our confidence in Arctic climate projections. Here we analyze the relationship between sea ice, cloud phase and surface radiation over the Arctic, defined as north of 60°N, using active- and passive-sensor satellite observations from three different datasets. We find that all datasets agree on the climatology and seasonal variability of total and liquid-bearing (liquid and mixed-phase) cloud covers. Similarly, our results show a robust relationship between decreased SIC and increased liquid-bearing clouds in the lowest levels (below 3 km) for all seasons but summer, while increased SIC and ice clouds are positively correlated in two of the three datasets. A refined spatial correlation analysis indicates that the relationship between SIC and liquid-bearing clouds can change sign over the Bering, Barent and Laptev seas, likely because of intrusions of warm air from low latitudes during winter and spring. Finally, the increase of liquid clouds resulting from decreasing SIC is associated with enhanced radiative cooling at the surface, which should contribute to dampening future Arctic surface warming as SIC continues to decline.

1 Introduction

Clouds can have different radiative effects over the Arctic (Curry et al. (1996); Shupe and Intrieri (2004)): cooling in summer generated by sunlight reflection and warming in winter through LW radiative heating of the surface. In a region where the warming can be up to four times larger than in the rest of the world (Boeke and Taylor (2018)), it is crucial to determine how clouds respond to climate change and whether their feedback will enhance or dampen the warming. While cloud feedback was shown to play a minor role in polar amplification in CMIP5 (Pithan and Mauritsen (2014)), studies using the most recent climate model generation (CMIP6) unveil a strong impact of extratropical mixed-phase clouds on global climate (Zelinka et al. (2020)). Part of the uncertainty in determining cloud variability in polar regions stems from the extent to which Arctic clouds respond to sea ice loss (Kay and Gettelman (2009); Morrison et al. (2018); Taylor and Monroe (2023)), which is still debated. Within the context of substantial decrease of sea ice extent over the past few decades (Kim et al., 2023), determining how clouds may be affected by this tremendous change is necessary to simulate realistic projections of polar climate.

https://doi.org/10.5194/egusphere-2023-2940
Preprint. Discussion started: 11 December 2023

The analysis of various observational datasets has led to consensus on the sensitivity of cloud fraction to sea-ice extent variability in the fall but not in the summer (e.g., (Kay and Gettelman (2009); Morrison et al. (2018)). As the sea-ice cover (SIC) decreases in the fall, the cloud fraction increases, mostly attributable to low-level liquid clouds (Morrison et al. (2018)). A more recent study found a larger cloud fraction over open ocean than over sea ice also in winter and spring (Taylor and Monroe (2023)). In general, these studies focus on one specific dataset over a limited amount of years, and disregard the response of ice clouds and more broadly free-troposphere clouds, which can have a notable radiative impact (L'Ecuyer et al. (2019)).

In this study, we use cloud observations from three different datasets that discriminate between liquid, ice and mixed-phase clouds. The first dataset is constrained to years 2007-2010 and is based on CloudSat-CALIPSO retrievals (DARDAR). The second is a new dataset based on CALIPSO-GOCCP that documents all liquid, mixed-phase and ice-only clouds from 2007 to 2020. The third is a passive-sensor satellite dataset based on MODIS retrievals (CERES) and also provides surface flux retrievals. We also analyze all seasons over the whole Arctic Ocean. After describing the datasets, we show their climatology of the different Arctic cloud types for all seasons. We then perform a correlation analysis of the SIC with all cloud types. Additionally, we focus on the vertical structure of these cloud types as a function of sea-ice conditions. Finally, we investigate the radiative impact of these clouds at the surface.

2 Datasets

2.1 CALIPSO-PHACT

The PHAse Cloud Type (PHACT) product development has been guided by recent ground-based observations to document the topmost liquid-bearing cloud layers for different cloud types (ice over liquid, liquid only, liquid seeded by ice above, mixed-phase, multilayer and single layer etc.) and for thin (optical depth $\lesssim 3$) and opaque (optical depth $\gtrsim 3$) clouds. PHACT, which will be described in a separate paper, uses instantaneous CALIPSO-GOCCP profiles (Cesana and Chepfer (2013)); Chepfer et al. (2010)). These profiles document cloud properties obtained from near-nadir lidar profiles at a 333 m along-track resolution and for 480 m altitude bins. Cloud phase diagnostics are based on the cloud particle sphericity instead of temperature, in contrast with many passive sensors. Liquid- and ice-dominated altitude bins are discriminated using the polarization state of the laser return, which changes when backscattered by a non-spherical crystal as opposed to spherical droplets. In highly reflective layers, the distinction between the two water phases is more ambiguous, because of multiple scattering and noise, and results in undefined-phase clouds, which often correspond to mixed-phase clouds (Cesana et al. (2016)).

PHACT differs from CALIPSO-GOCCP cloud phase statistics in two main ways. First, PHACT provides ice-only (no liquid in the column) and mixed-phase (liquid with ice below, contiguous or not) cloud covers, in addition to the traditional liquid (with possibly ice above) phase category. Second, the phase cloud cover is computed as the number of ice, liquid or mixed-phase cloudy profiles divided by the total number of profiles, consistent with the common definition of cloud cover:

$$CC_{phase} = N_{phase}/N_{profiles} \quad (1)$$

https://doi.org/10.5194/egusphere-2023-2940
Preprint. Discussion started: 11 December 2023

Where phase means either ice, liquid or mixed-phase.

As a result, the sum of ice-only, liquid, and mixed-phase cloud covers cannot be greater than 1. We note a large difference in the magnitude of the vertical cloud profiles between CALIPSO-GOCCP and PHACT because PHACT is focused on the topmost liquid-layer whereas CALIPSO-GOCCP documents all available vertical levels. A validation study against in situ aircraft measurements shows that the maximum disagreement fraction between CALIPSO-GOCCP instantaneous profiles – used in PHACT – and five in situ aircraft flights is ~ 20 % (Cesana et al. (2016); their Table 3).

2.2 CloudSat-CALIPSO DARDAR

The DARDAR product (liDAR/raDAR; Delanoë and Hogan (2010)) uses both CALIPSO and CloudSat observations to retrieve vertical profiles of cloud properties with a vertical and horizontal resolution of 60 m and 1.7 km, respectively. The DARDAR cloud phase algorithm is based on the complementarity of the high sensitivity of the 532 nm lidar to small and spherical liquid droplets and the 94 GHz radar to large ice crystals. In addition, the algorithm also uses cloudy layer temperature and cloud geometrical thickness to determine cloud phase. DARDAR distinguishes between ice, mixed, supercooled and warm liquid clouds. A more detailed explanation of the algorithm is given by Mioche et al. (2015). Since DARDAR is not provided as a gridded Level3 product (as opposed to CALIPSO-GOCCP, CALIPSO-PHACT and CERES), we have processed the vertical profiles for the available time period, computed the cloud phase covers following the same definition as CALIPSO-PHACT and computed pan-Arctic statistics onto a 2.5°x2.5° grid. Similarly, we have used a cloud phase classification for the 2D maps so that the sum of ice-only, liquid and mixed-phase cloud covers cannot be greater than 1 and, hence, is equal to the total cloud cover. Should we have used ice-containing and liquid-containing 2D cloud covers we could have accounted for liquid or ice two times in the same profile, hence a cloud cover greater than 1.

We are not aware of a formal evaluation of DARDAR product but we note that when the lidar signal is fully attenuated (i.e., no more signal), the DARDAR algorithm attributes the ice phase to any cloudy pixels at subfreezing temperatures, which may lead to an overestimate of the ice cloud covers. In addition, Mioche et al. (2015) mention a potential overestimate of mixed-phase cloud due to excessive supercooled liquid detections, which may have been mitigated in the newer version of DARDAR product, which is used here.

2.3 CERES

To study the surface fluxes, we use Clouds and the Earth's Radiant Energy System (CERES) FluxByCldTyp – Level 3 (Sun et al. (2022)), which also contains information about the cloud phase. The cloud and cloud phase information is based on MODIS cloud properties. The phase is retrieved for daytime only using the newest MODIS collection 6 (MODIS-C6) cloud phase algorithm, which employed a decision tree logic based on four independent tests (Marchant et al. (2016)): cloud top temperature, tri-spectral infrared test using difference in brightness temperatures, a 1.38μm test to determine the presence of cirrus clouds and a tri-spectral cloud effective radius test. We note that MODIS-C6 cloud phase has a large agreement fraction with CALIPSO science team cloud phase retrievals (up to 90%, Marchant et al. (2016)) and that the use of daytime-only observations is a limiting factor in our analysis (no cloud phase data during the Arctic winter).

https://doi.org/10.5194/egusphere-2023-2940
Preprint. Discussion started: 11 December 2023

We use data from the 2007-2020 overlapping period for PHACT and CERES. DARDAR data is available for 2007-2010 and 2013-2017, however, this latter period is limited to daytime observations, and using it could introduce biases in the comparison. Although DARDAR 2013-2017 and 2007-2010 shows differences in the total cloud cover that are comparable to that of PHACT over the same time periods (Fig. S1 and S2, bottom right plots), major differences appear in DARDAR cloud phase partitioning that do not in PHACT (Fig. S1 and S2, bottom rows). These differences suggest that using daytime-only data has a strong impact on DARDAR phase diagnostics. Finally, all datasets are projected onto a 2.5˚x2.5˚ grid.

3 Results

Figure 1 shows a comparison of ice, liquid, mixed-phase and total cloud covers for all the datasets. All three datasets agree very well on the total cloud cover with a sharp contrast between land and sea and maxima over the Laptev, Barent and Greenland seas. Interestingly, the datasets also detect a very similar liquid cloud cover (in terms of means and pattern correlations, Table 1 and Fig. S3), even though they use independent methods to retrieve liquid layers. We note that CERES exhibits the largest amount of liquid clouds for two reasons (47%). First, it does not distinguish between mixed-phase and liquid clouds and second, it doesn't include the winter season north of 70˚N, which is the season with the least liquid cloud amount (Cesana et al. (2012), their Fig. 1). When accounting for all liquid-bearing clouds (i.e., liquid-only and mixed-phase clouds), the differences among datasets drastically lessens: 53%, 51% and 47% for DARDAR, PHACT and CERES, respectively. The mixed-phase cloud category is also consistent between DARDAR and PHACT (pattern correlation r = 0.56). Yet DARDAR diagnoses slightly more mixed-phase clouds than PHACT (26% compared to 14%), likely because the radar is able to penetrate the clouds deeper and detect precipitating ice below. In this regard, PHACT can be viewed as a lower bound in terms of mixed-phase cloud cover. On average, these mixed-phase clouds account for about 26% of liquid-bearing clouds in PHACT and 49% in DARDAR (Fig. S4, Tab. S1), which is closer to 73% from Arctic ground-based measurements using a radar with a cloud detection sensibility similar to CloudSat (Silber et al. (2021)). Finally, the greatest differences between the datasets in terms of pattern correlation and cloud covers come from the ice clouds. DARDAR and CERES showmore ice clouds than PHACT, and their pattern correlation are smaller than those from liquid clouds. To diagnose cloud cover, the DARDAR algorithm uses CALIPSO level2 product, which averages the lidar signal along track up to 80 km to be able to retrieve the thinnest cirrus clouds. This may explain why DARDAR detects more ice clouds than PHACT – although they both use CALIPSO observations but may also cause false positive detections (Cesana et al. (2016)).

Figure 2 shows the seasonal variability of each cloud type over the Arctic for the three datasets. All datasets exhibit a maximum in Fall and a minimum in Winter in the total cloud cover, mostly driven by liquid-containing clouds (liquid and mixed-phase), which is consistent with previous findings (e.g., Cesana et al. (2012); Mioche et al. (2015)). As expected, ice cloud cover reaches its lowest value in summer (July) in all datasets, while its maximum occurs in the winter.

Next, we explore the relationship between clouds and SIC variability. Given the relatively good agreement in the representation of the seasonal variability of liquid and total cloud covers between all datasets, we expect to find robust relationships between these clouds and SIC.

https://doi.org/10.5194/egusphere-2023-2940
Preprint. Discussion started: 11 December 2023

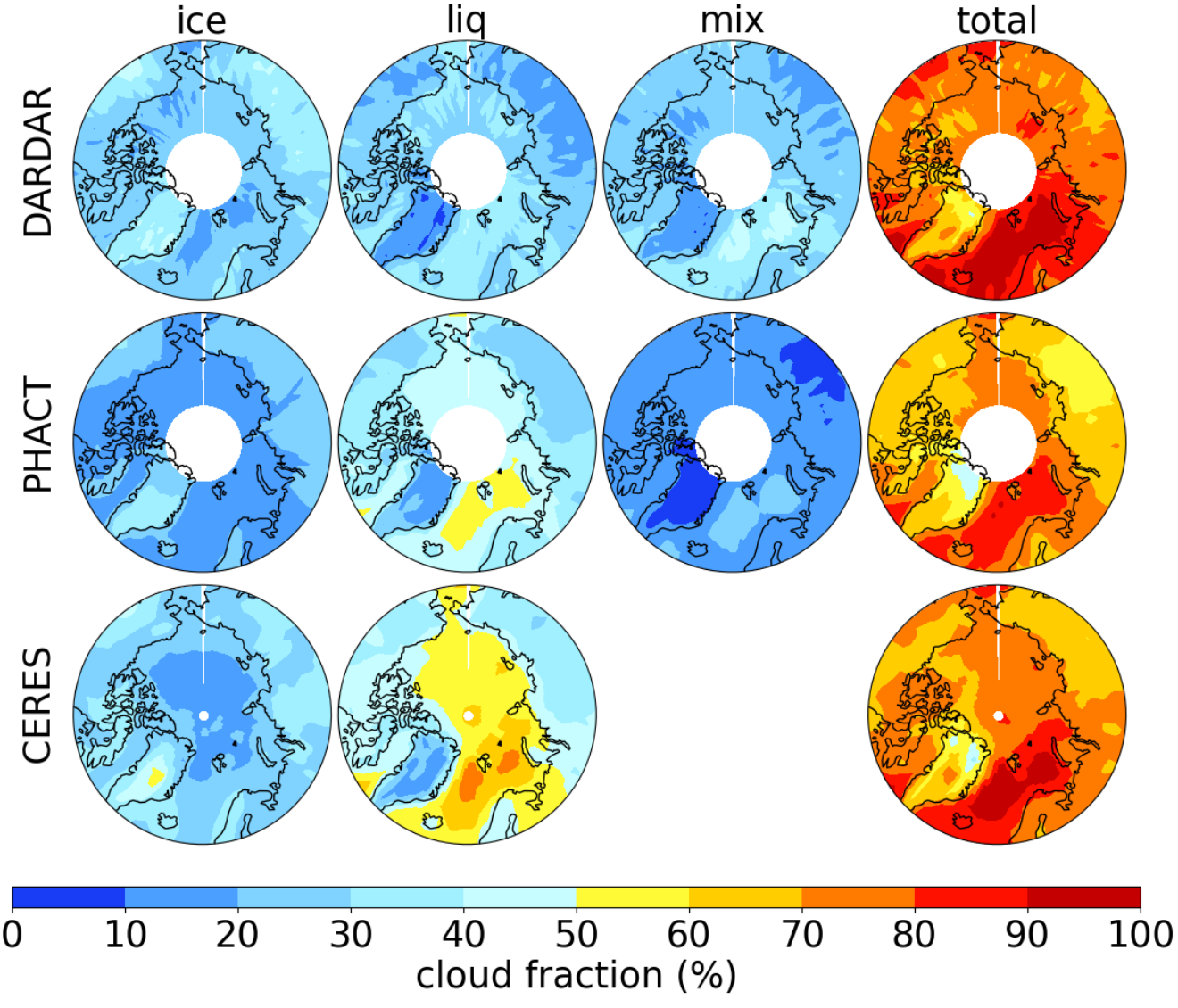

Figure 1. Average cloud ice, liquid, mixed-phase and total cloud covers (%) for DARDAR (2007-2010; Delanoë and Hogan (2010)), PHACT (2007-2020) and CERES (2007-2020; Sun et al. (2022)).

https://doi.org/10.5194/egusphere-2023-2940
Preprint. Discussion started: 11 December 2023

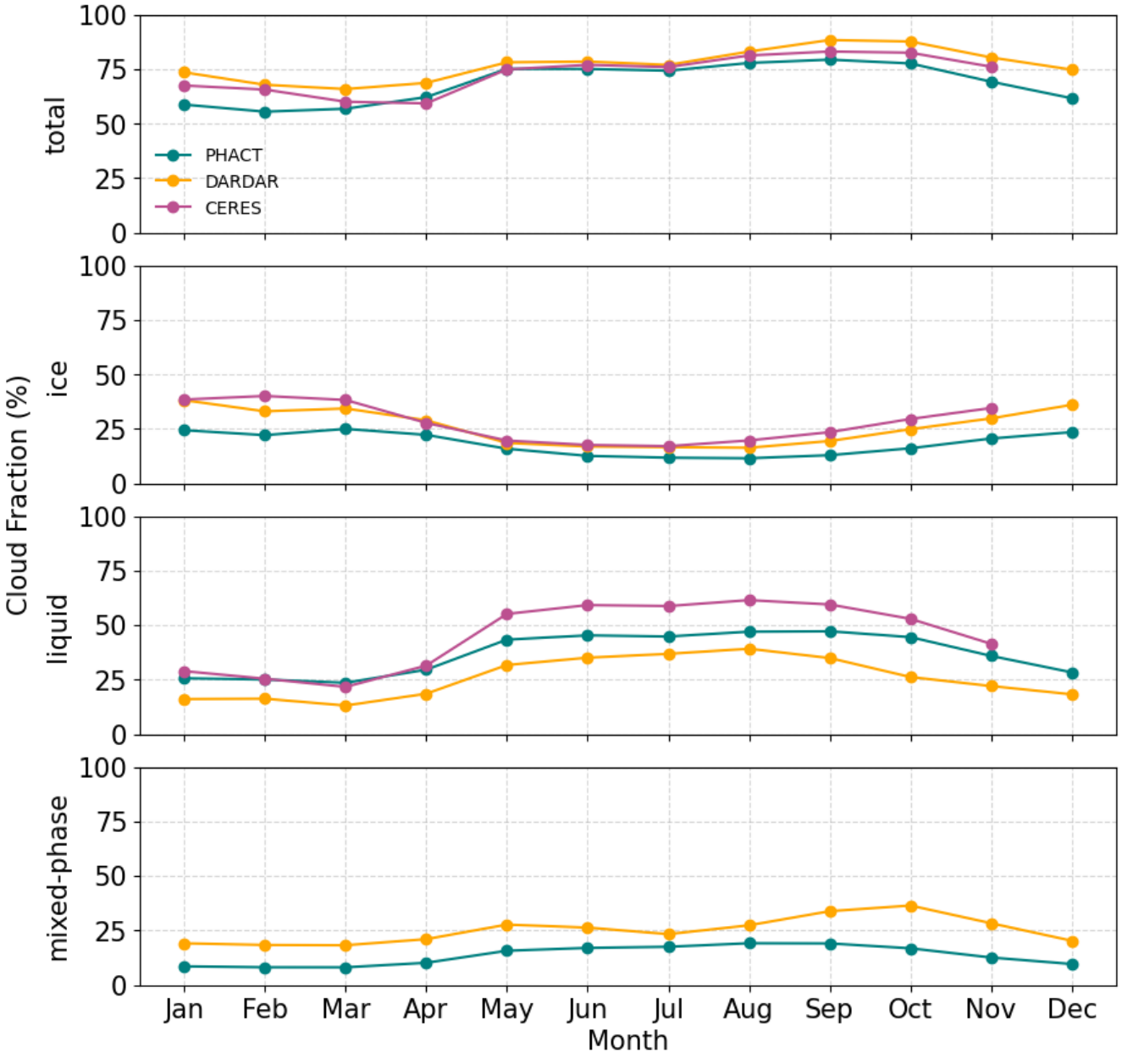

Figure 2. Seasonal variability of the Arctic cloud cover (%) for DARDAR (orange, 2007-2010), CERES (purple, 2007-2020) and PHACT (green, 2007-2020).

https://doi.org/10.5194/egusphere-2023-2940
Preprint. Discussion started: 11 December 2023

Figure 3. Colored table of correlations between cloud types and SIC for all seasons and for DARDAR (2007-2010), PHACT (2007-2020) and CERES (2007-2020). Dark red and blue colors indicate strong correlations and anti-correlations, respectively.

https://doi.org/10.5194/egusphere-2023-2940
Preprint. Discussion started: 11 December 2023

Table 1. Arctic mean cloud covers (%) for all datasets from 2007-2010. We note a robust consistency in the liquid-bearing cloud cover among all datasets.

(%)	**DARDAR**	**PHACT**	**CERES** (< 82°N)	**CERES**
Total	77	68	73	73
Ice	26	17	26	24
Liquid	26	37	47	49
Mixed	25	14	N/A	N/A
Liquid-bearing	51	51	47	49

We compute correlations between SIC and cloud covers from each cloud type for our three cloud datasets. Our SIC comes from ERA5 reanalysis, but we note that no substantial differences are found using a different dataset (Hadley Centre Sea Ice and Sea Surface Temperature, not shown). Furthermore, we focus on those grid boxes in which SIC varies over the time period, that is averaged SIC is greater than 0.01 and smaller than 0.99. Our results are consistent with previous literature. We find large and significant negative correlations between SIC and liquid and total cloud covers from all datasets (Fig. 3). In addition, our results show little to no correlation between SIC and liquid cloud cover for the summer, consistent with previous studies (Kay and Gettelman (2009); Morrison et al. (2018)). More surprisingly, our analysis indicates that the ice cloud cover is positively correlated with SIC in all datasets, which, to our knowledge, hasn't been reported in the literature before. It is also interesting to note that these correlations are weaker when using all grid boxes rather than first averaging across the Arctic. This discrepancy might be indicative of regional variability, which fades out when looking at a pan-Arctic perspective.

The correlation maps help us better understand the variability of the relationships between each cloud type and SIC as a function of the seasons (Figs. 4-5-6). For liquid clouds, the correlations are generally negative in the fall and spring while in summer little correlation is found, and in winter, it is mostly negative except over the Bering, Barent and Laptev seas. This exception might be explained by the incursion of moist and warm air from the Aleutian low – a frequent large-scale atmospheric pattern during the Arctic cold season (Overland et al. (1998)). The advection of moist air strongly affects Arctic surface temperatures (Shulski et al. (2010)). This moist air incursion results in the formation of liquid clouds at subfreezing temperatures in that area, while the sea ice continues to build up, even though strong Aleutian lows can reduce sea-ice growth (Walsh et al. (2017), Dörr et al. (2021)). We find similar patterns for the mixed-phase and total cloud correlation maps, which are clearly dominated by the response of liquid-containing clouds (liquid-only and mixed-phase clouds). The results are more diverse among the datasets when it comes to ice clouds. The correlations are mostly positive in DARDAR and PHACT (except in winter) and both negative and positive depending on the season in CERES. Ice clouds may have two distinct origins: high cirrus clouds mostly controlled by synoptic-scale dynamics through so-called intrusions from lower latitudes (Pithan et al. (2018)), and low and mid-level ice clouds driven by either small convective pockets or local increases in moisture fluxes, which

https://doi.org/10.5194/egusphere-2023-2940
Preprint. Discussion started: 11 December 2023

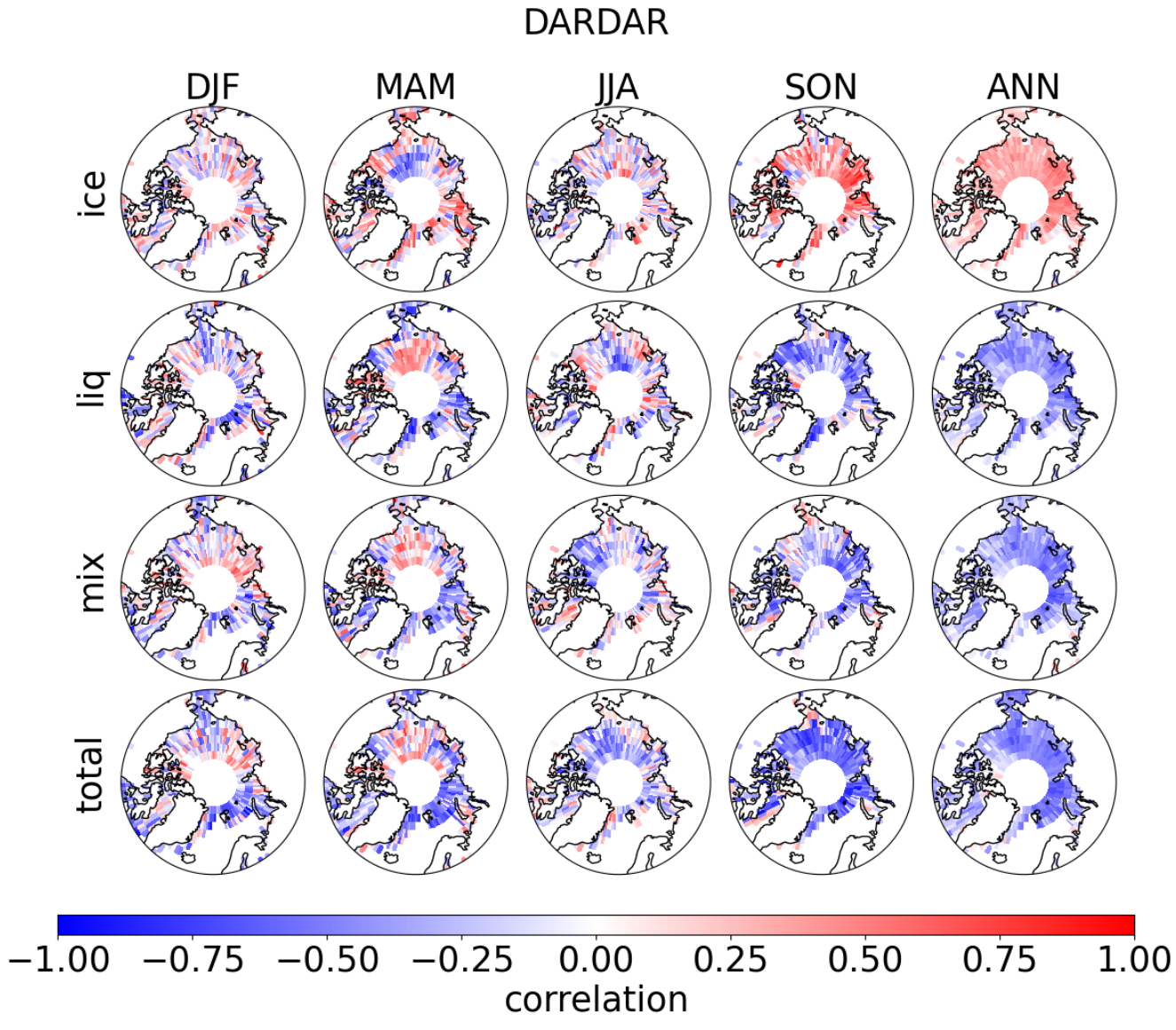

Figure 4. Maps of correlations between DARDAR cloud types and SIC for each season (2007-2010).

https://doi.org/10.5194/egusphere-2023-2940
Preprint. Discussion started: 11 December 2023

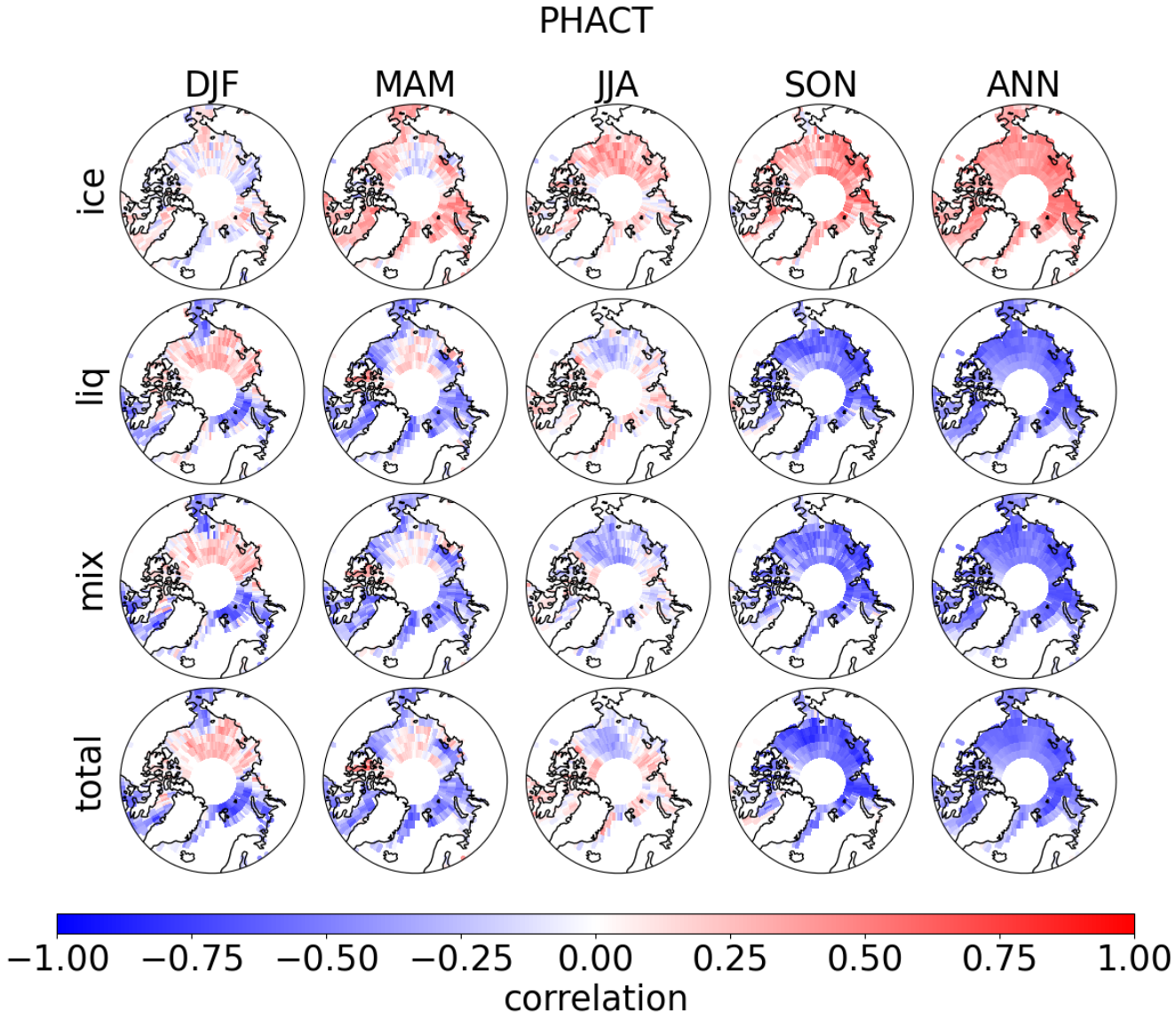

Figure 5. Maps of correlations between PHACT cloud types and SIC for each season (2007-2020).

https://doi.org/10.5194/egusphere-2023-2940
Preprint. Discussion started: 11 December 2023

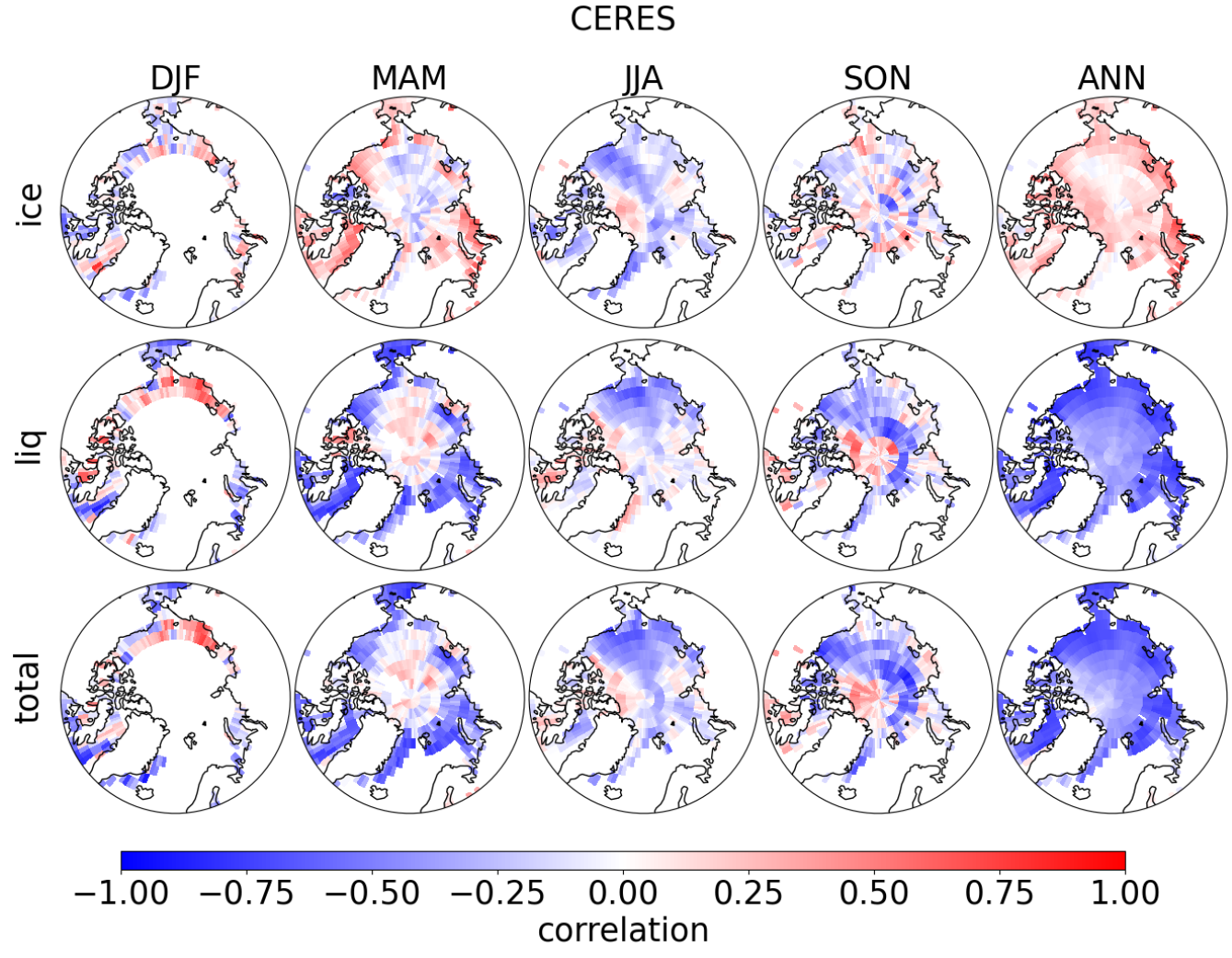

Figure 6. Maps of correlations between CERES cloud types and SIC for each season (2007-2020).

https://doi.org/10.5194/egusphere-2023-2940
Preprint. Discussion started: 11 December 2023

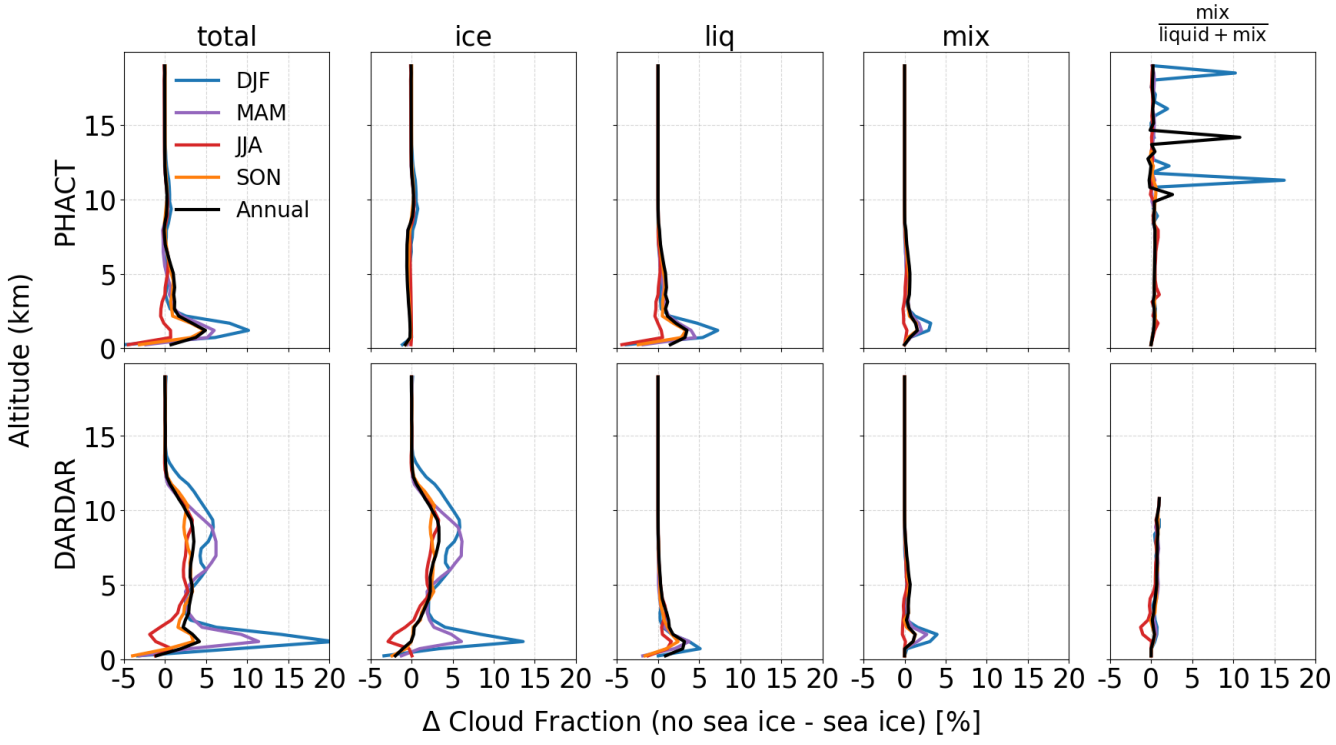

Figure 7. Effect of sea-ice conditions on cloud type profiles (%) for PHACT (top, 2007-2020) and DARDAR (bottom, 2007-2010)

form liquid clouds first and then ice clouds (Pithan et al. (2018)). Over sea ice, both of these processes might be enhanced since the air is generally colder, explaining positive correlations between ice clouds and sea ice.

Next, we take advantage of the active-sensor profiling capability to investigate changes in each cloud-type profile as a function of the surface conditions to determine what altitude contributes the most to cloud variability (Fig. 7). Here we compute the difference of cloud type profiles above open-ocean minus sea-ice covered grid boxes, where an open-ocean and sea-ice grid box is defined as SIC < 0.4 and SIC > 0.6, respectively, in order to maximize the number of grid boxes utilized in the computation. These results are consistent with our correlation analysis and provide additional insights. The cloud cover change is mostly driven by liquid clouds and the mixed-phase clouds behave like the liquid clouds, which increase over open ocean during all seasons but summer. Unsurprisingly, the boundary layer is the main contributor to the change although right above it, the change is not negligible. However, the ice cloud cover increase over sea ice is more subtle and results from compensating effects: an increase of the ice cloud cover below 8 km that surpasses the decrease higher up. It is interesting to note that the increase of high ice clouds (above 8km) over open ocean is apparent in all seasons, which could be due to constant local transport of moisture fluxes in the high levels due to higher open-ocean surface temperatures.

Finally, in order to determine the radiative impact of these cloud changes, we compute net surface LW, SW and total CRE for open-ocean and sea-ice-covered conditions following the same method as described in the above paragraph (Table 2). Our

https://doi.org/10.5194/egusphere-2023-2940
Preprint. Discussion started: 11 December 2023

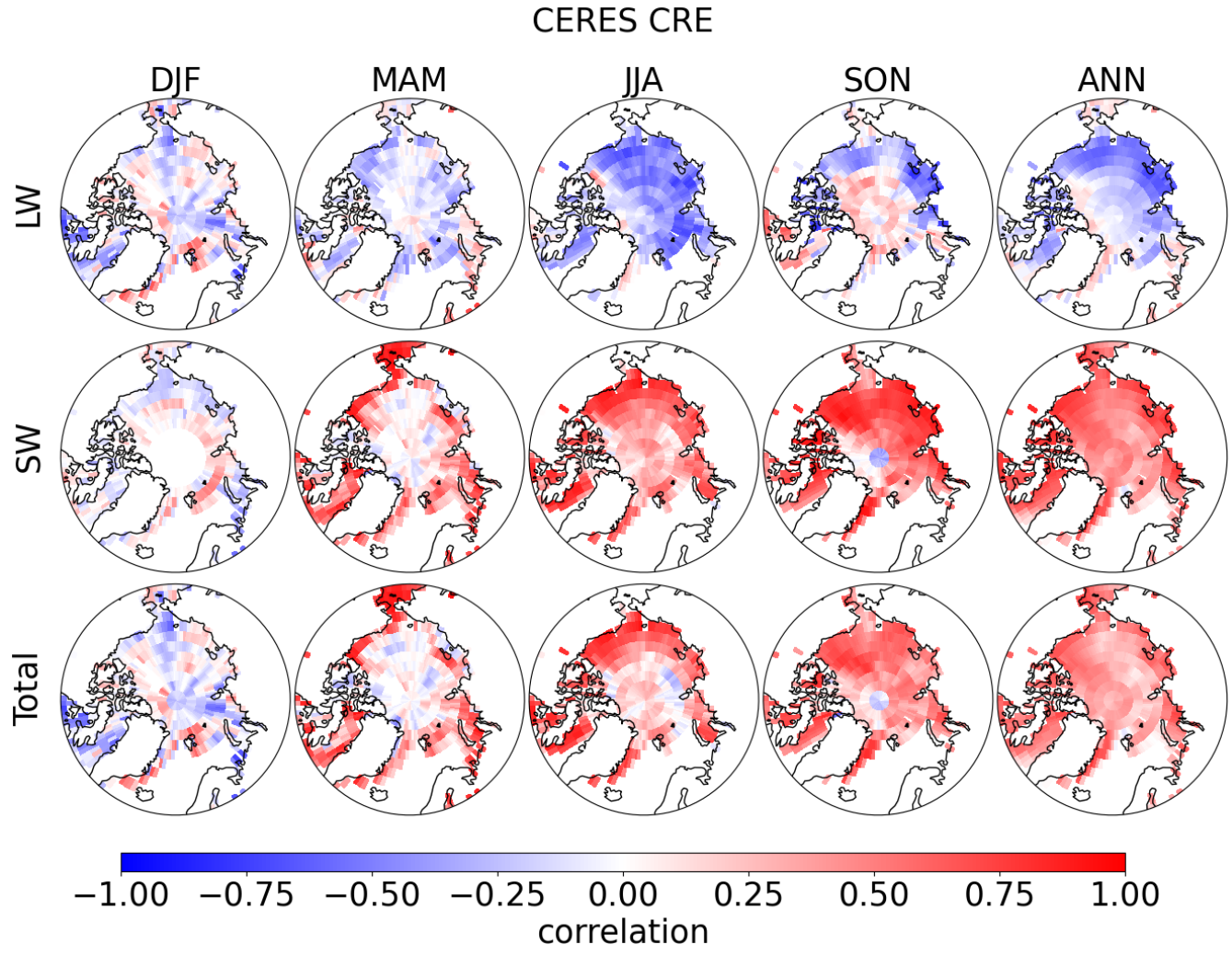

Figure 8. Maps of correlations between CERES surface net cloud radiative effects and SIC for each season (2007-2020).

https://doi.org/10.5194/egusphere-2023-2940
Preprint. Discussion started: 11 December 2023

Table 2. Changes in longwave, shortwave, and net surface cloud radiative effects (Wm^{-2}) between open-ocean and sea-ice grid boxes (CERES, 2007-2020).

(Wm^{-2})	**DJF**	**MAM**	**JJA**	**SON**	**ANN**
$\Delta LWCRE$	4.9	7.2	3.4	-0.2	4.8
$\Delta SWCRE$	-3	-47.7	-37.2	-20.7	-31.4
$\Delta TotalCRE$	1.9	-40.6	-33.8	-20.9	-26.6

results indicate that the increase of cloud cover over open ocean, driven by low-level liquid clouds, corresponds to stronger cooling in all seasons but winter, attributable to larger SW reflection than LW absorption. The correlation maps between SIC and the net effect of the clouds at the surface (Fig. 8) are consistent with the correlations found between SIC and liquid cloud covers, albeit of opposite sign. On the one hand, SIC is positively correlated with net SW CRE at the surface because the reduction in liquid clouds generated by increased SIC allows more SW radiation to be absorbed. On the other hand, fewer liquid clouds also reduce the net LW CRE warming at the surface, resulting in a negative correlation of net LW CRE and SIC. Yet we note that even when the correlation between clouds and SIC is low (e.g., in summer, fig. 6), the correlation between net CRE and SIC remains high, emphasizing the importance of the underlying surface type for surface CRE. Finally, our results show that the correlation of the net total CRE with sea ice is dominated by the SW component for all seasons but winter.

4 Summary and discussion

Using three independent active- and passive-sensor satellite datasets from the A-train, we analyze the relationship between sea ice, cloud phase and surface radiation over the Arctic (north of 60˚N). We find that all three satellite datasets depict a similar pattern and seasonal variability of total and liquid-bearing cloud covers while DARDAR diagnoses far more ice clouds with distinct seasonal variability compared to PHACT and CERES. We then show that the strong negative correlation between Arctic cloud cover and sea ice cover (SIC) is primarily driven by liquid-bearing clouds from the lowest levels (i.e., below 3 km), for which mixed-phase clouds account for 26 % in PHACT. This relationship is robust among all satellite observations for all seasons but summer, which is consistent with findings from previous studies using CALIPSO liquid 3D cloud fraction (Morrison et al. (2018)) and CALIPSO-CloudSat total 3D cloud fraction (Taylor and Monroe (2023)). Additionally, our seasonal maps of correlation reveal the presence of regional differences, which may be driven by local processes and synoptic circulation. In particular over the Bering, Barent and Laptev seas, where winter and spring intrusions of low-latitude warm air change the sign of the correlation between liquid cloud cover and SIC. Furthermore, we show that ice-only clouds also correlate well with SIC, which hasn't been reported in the literature to our knowledge. Finally, the increase of liquid-bearing clouds with open-ocean conditions – and to some extent the decrease of ice clouds – is associated with more radiative cooling

https://doi.org/10.5194/egusphere-2023-2940
Preprint. Discussion started: 11 December 2023

from clouds at the surface, attributable to a larger SW CRE cooling than LW CRE warming. Such a cooling effect is found in all seasons but winter, when the LW CRE warming exceeds the SW CRE cooling.

In response to climate warming, Arctic SIC declines and will most likely continue to do so in the future, with ice-free summers that could occur as early as 2030 (Kim et al. (2023)). Within this context, it is important to quantify the effect of sea-ice loss on clouds, which are a major contributor to surface radiative budget. Our analysis suggests that optically thick low-level liquid clouds will be more frequent as SIC declines, and this process should contribute to mitigating Arctic surface warming, except in winter. These results could be used to assess the SIC-cloud relationship in climate models, which still struggle to represent cloud phase transition (Cesana et al. (2022)), and thereby help narrow down the large uncertainties in their representation of Arctic amplification (Boeke and Taylor (2018)).

Data availability. The PHACT observations can be downloaded from zenodo link to add. The DARDAR instantaneous files were obtained from https://www.icare.univ-lille.fr/dardar/documentation-dardar-mask/ (restricted access) and the gridded statistics were computed from the ICARE Data and Service Center and can be downloaded from zenodo link to add . The CERES cloud phase and flux observations were downloaded from the following CERES websites https://ceres-tool.larc.nasa.gov/ord-tool/jsp/FluxByCldTypSelection.jsp and https://ceres-tool.larc.nasa.gov/ord-tool/jsp/SYN1degEd41Selection.jsp, respectively. The ERA5 monthly means of sea-ice cover were downloaded from the Climate Data Store website (https://cds.climate.copernicus.eu/cdsapp#!/dataset/reanalysis-era5-pressure-levels-monthly-means?tab=form).

Author contributions. GC designed the study, carried out the analysis, processed PHACT data, and drafted the figures. OP and LV processed the DARDAR and CERES datasets. OP finalized the processing of DARDAR data and prepared the figures and tables. GC wrote the manuscript with contributions from all co-authors.

Competing interests. The authors declare that they have no conflict of interest.

Acknowledgements. GC, MO and ZJ were supported by National Aeronautics and Space Administration IDS (Interdisciplinary Research in Earth Science) (80NSSC20K1523) (award 19-IDS19-0059). GC was also supported by a CloudSat-CALIPSO RTOP at the NASA Goddard Institute for Space Studies and by the U.S. Department of Energy's (DOE) Atmospheric System Research, an Office of Science Biological and Environmental Research program, under grant DE-SC0021004. We would also like to thank the NASA Office of STEM Engagement at GISS, the Minority University Research and Education Project (MUREP), and the NASA OSTEM Internship program, for the support offered to OP and LV. Resources supporting this work were provided by the NASA Center for Climate Simulation (NCCS) at Goddard Space Flight Center. We thank NASA and CNES for giving access to CALIPSO observations, and Climserv for giving access to CALIPSO-GOCCP observations and for providing computing resources.

https://doi.org/10.5194/egusphere-2023-2940
Preprint. Discussion started: 11 December 2023

References

Boeke, R. C. and Taylor, P. C.: Seasonal energy exchange in sea ice retreat regions contributes to differences in projected Arctic warming, Nature Communications, 9, https://doi.org/10.1038/s41467-018-07061-9, 2018.

Cesana and Chepfer, H.: Evaluation of the cloud thermodynamic phase in a climate model using CALIPSO-GOCCP, Journal of Geophysical Research: Atmospheres, 118, 7922–7937, https://doi.org/10.1002/jgrd.50376, 2013.

Cesana, G., Kay, J. E., Chepfer, H., English, J. M., and de Boer, G.: Ubiquitous low-level liquid-containing Arctic clouds: New observations and climate model constraints from CALIPSO-GOCCP, Geophysical Research Letters, 39, 1–6, https://doi.org/10.1029/2012GL053385, 2012.

Cesana, G., Chepfer, H., Winker, D., Getzewich, B., Cai, X., Jourdan, O., Mioche, G., Okamoto, H., Hagihara, Y., Noel, V., and Reverdy, M.: Using in situ airborne measurements to evaluate three cloud phase products derived from CALIPSO, Journal of Geophysical Research, 121, 5788–5808, https://doi.org/10.1002/2015JD024334, 2016.

Cesana, G. V., Khadir, T., Chepfer, H., and Chiriaco, M.: Southern Ocean Solar Reflection Biases in CMIP6 Models Linked to Cloud Phase and Vertical Structure Representations, Geophysical Research Letters, 49, e2022GL099 777, https://doi.org/https://doi.org/10.1029/2022GL099777, e2022GL099777 2022GL099777, 2022.

Chepfer, H., Bony, S., Winker, D., Cesana, G., Dufresne, J. L., Minnis, P., Stubenrauch, C. J., and Zeng, S.: The GCM-Oriented CALIPSO Cloud Product (CALIPSO-GOCCP), Journal of Geophysical Research, 115, D00H16, https://doi.org/10.1029/2009JD012251, 2010.

Curry, J. A., Schramm, J. L., Rossow, W. B., and Randall, D.: Overview of Arctic Cloud and Radiation Characteristics, Journal of Climate, 9, 1731–1764, https://doi.org/10.1175/1520-0442(1996)009<1731:OOACAR>2.0.CO;2, 1996.

Delanoë, J. and Hogan, R. J.: Combined CloudSat-CALIPSO-MODIS retrievals of the properties of ice clouds, Journal of Geophysical Research: Atmospheres, 115, https://doi.org/https://doi.org/10.1029/2009JD012346, 2010.

Dörr, J., Årthun, M., Eldevik, T., and Madonna, E.: Mechanisms of Regional Winter Sea-Ice Variability in a Warming Arctic, Journal of Climate, 34, 8635 – 8653, https://doi.org/https://doi.org/10.1175/JCLI-D-21-0149.1, 2021.

Kay, J. E. and Gettelman, A.: Cloud influence on and response to seasonal Arctic sea ice loss, Journal of Geophysical Research Atmospheres, 114, 1–18, https://doi.org/10.1029/2009JD011773, 2009.

Kim, Y.-H., Min, S.-K., Gillett, N. P., Notz, D., and Malinina, E.: Observationally-constrained projections of an ice-free Arctic even under a low emission scenario, Nature Communications, 14, 3139, https://doi.org/10.1038/s41467-023-38511-8, 2023.

L'Ecuyer, T. S., Hang, Y., Matus, A. V., and Wang, Z.: Reassessing the Effect of Cloud Type on Earth's Energy Balance in the Age of Active Spaceborne Observations. Part I: Top of Atmosphere and Surface, Journal of Climate, 32, 6197 – 6217, https://doi.org/https://doi.org/10.1175/JCLI-D-18-0753.1, 2019.

Marchant, B., Platnick, S., Meyer, K., Arnold, G. T., and Riedi, J.: MODIS Collection 6 shortwave-derived cloud phase classification algorithm and comparisons with CALIOP, Atmospheric Measurement Techniques, 9, 1587–1599, https://doi.org/10.5194/amt-9-1587-2016, 2016.

Mioche, G., Jourdan, O., Ceccaldi, M., and Delanoë, J.: Variability of mixed-phase clouds in the Arctic with a focus on the Svalbard region: A study based on spaceborne active remote sensing, Atmospheric Chemistry and Physics, 15, 2445–2461, https://doi.org/10.5194/acp-15-2445-2015, 2015.

https://doi.org/10.5194/egusphere-2023-2940
Preprint. Discussion started: 11 December 2023

Morrison, A. L., Kay, J. E., Chepfer, H., Guzman, R., and Yettella, V.: Isolating the Liquid Cloud Response to Recent Arctic Sea Ice Variability Using Spaceborne Lidar Observations, Journal of Geophysical Research: Atmospheres, 123, 473–490, https://doi.org/https://doi.org/10.1002/2017JD027248, 2018.

Overland, J. E., Miletta, J., Adams, , and Bond, N. A.: Decadal Variability of the Aleutian Low and Its Relation to High-Latitude Circulation*, 1998.

Pithan, F. and Mauritsen, T.: Arctic amplification dominated by temperature feedbacks in contemporary climate models, Nature Geoscience, 7, 181–184, https://doi.org/10.1038/ngeo2071, 2014.

Pithan, F., Svensson, G., Caballero, R., Chechin, D., Cronin, T. W., Ekman, A. M. L., Neggers, R., Shupe, M. D., Solomon, A., Tjernström, M., and Wendisch, M.: Role of air-mass transformations in exchange between the Arctic and mid-latitudes, Nature Geoscience, 11, 805–812, https://doi.org/10.1038/s41561-018-0234-1, 2018.

Shulski, M., Walsh, J., Stevens, E., and Thoman, R.: Diagnosis of extended cold-season temperature Anomalies in Alaska, Monthly Weather Review, 138, 453–462, https://doi.org/10.1175/2009MWR3039.1, 2010.

Shupe, M. D. and Intrieri, J. M.: Cloud Radiative Forcing of the Arctic Surface: The Influence of Cloud Properties, Surface Albedo, and Solar Zenith Angle, Journal of Climate, 17, 616–628, https://doi.org/10.1175/1520-0442(2004)017<0616:CRFOTA>2.0.CO;2, 2004.

Silber, I., Fridlind, A. M., Verlinde, J., Ackerman, A. S., Cesana, G. V., and Knopf, D. A.: The prevalence of precipitation from polar supercooled clouds, Atmospheric Chemistry and Physics, 21, 3949–3971, https://doi.org/10.5194/acp-21-3949-2021, 2021.

Sun, M., Doelling, D. R., Loeb, N. G., Scott, R. C., Wilkins, J., Nguyen, L. T., and Mlynczak, P.: Clouds and the Earth's Radiant Energy System (CERES) FluxByCldTyp Edition 4 Data Product, Journal of Atmospheric and Oceanic Technology, 39, 303 – 318, https://doi.org/https://doi.org/10.1175/JTECH-D-21-0029.1, 2022.

Taylor, P. C. and Monroe, E.: Isolating the Surface Type Influence on Arctic Low-Clouds, Journal of Geophysical Research: Atmospheres, 128, e2022JD038 098, https://doi.org/https://doi.org/10.1029/2022JD038098, e2022JD038098 2022JD038098, 2023.

Walsh, J. E., Bieniek, P. A., Brettschneider, B., Euskirchen, E. S., Lader, R., and Thoman, R. L.: The exceptionally warm winter of 2015/16 in Alaska, Journal of Climate, 30, 2069–2088, https://doi.org/10.1175/JCLI-D-16-0473.1, 2017.

Zelinka, M. D., Myers, T. A., McCoy, D. T., Po-Chedley, S., Caldwell, P. M., Ceppi, P., Klein, S. A., and Taylor, K. E.: Causes of Higher Climate Sensitivity in CMIP6 Models, Geophysical Research Letters, 47, 1–12, https://doi.org/10.1029/2019GL085782, 2020.